J Solid State Electrochem (2007) 11:1505–1510
DOI 10.1007/s10008-007-0338-9

ORIGINAL PAPER

# Electroactive LbL films of metallic phthalocyanines and poly(*o*-methoxyaniline) for sensing

**Amanda C. Santos · Valtencir Zucolotto · Carlos J. L. Constantino · Helder N. Cunha · José R. dos Santos Jr. · Carla Eiras**

Received: 31 January 2007 / Revised: 28 February 2007 / Accepted: 11 April 2007 / Published online: 8 May 2007


**Abstract** Multilayered nanostructured films have been widely investigated for electrochemical applications as modified electrodes, including the layer-by-layer (LbL) films where properties such as thickness and film architecture can be controlled at the molecular level. In this study, we investigate the electrochemical features of LbL films of poly (*o*-methoxyaniline; POMA) and tetrasulfonated phthalocyanines containing nickel (NiTsPc) or copper (CuTsPc). The films displayed well-defined electroactivity, with redox pairs at 156 and 347 mV vs SCE, characteristic of POMA, which allowed their use as modified electrodes for detecting dopamine and ascorbic acid at concentrations as low as $10^{-5}$ M.

**Keywords** LbL films · Dopamine · Ascorbic acid · Sensors · Phthalocyanines

This paper is dedicated to Prof. Francisco Nart, in memoriam.

A. C. Santos · J. R. dos Santos Jr. · C. Eiras (✉)
DQ, UFPI, CCN,
64049-550 Teresina, PI, Brazil
e-mail: eirasc@yahoo.com.br

V. Zucolotto
IFSC, USP, CP 369,
13560-970 São Carlos, SP, Brazil

C. J. L. Constantino
DFQB, FCT, UNESP, CP 467,
19060-900 Presidente Prudente, SP, Brazil

H. N. Cunha
DF, UFPI, CCN,
64049-550 Teresina, PI, Brazil

## Introduction

Nanostructured thin films have been widely used in sensing, especially because of the possibility of combining materials in a synergistic way where specific properties may be controlled at the molecular level [1, 2]. Organic–inorganic hybrid films are particularly interesting for sensing, as parameters such as the electronic properties of each material can be tuned to maximize interactions between film and analyte. This is the case of conducting polymers assembled with porphyrins and phthalocyanines used as modified electrodes for electrocatalysis and sensors [3, 4]. The activity of modified electrodes of polyaniline (PANI) and polypyrrole (PPY) containing metallic phthalocyanines in oxygen reduction, for example, was investigated by Coutanceau et al. [5]. They compared oxygen reduction rates between conducting polymers electrochemically synthesized in the presence of cobalt (CoTsPc) or iron (FeTsPc) tetrasulfonated phthalocyanines and a bare platinum electrode. Using a similar approach, Fuentes et al. [6] found that the control over film thickness was crucial to optimize the electrocatalytic properties of modified electrodes of PPY incorporating nickel tetrasulfonated phthalocyanine (NiTsPc). The modified electrodes displayed an electrocatalytic effect on the anodic oxidation of propylgalate in comparison to bare platinum electrodes.

Another efficient strategy to produce multilayered hybrid films is through the electrostatic layer-by-layer technique (LbL) [1], which is further advantageous owing to the experimental simplicity and possible assembly of materials directly from their aqueous solutions [7, 8]. In a previous study, our group produced LbL films made with parent PANI and phthalocyanines for dopamine (DA) and ascorbic acid (AA) sensing [9]. In this paper, we extend this investigation to analyze the physicochemical properties of LbL films of poly(-*o*-methoxyaniline; POMA) alternated

with tetrasulfonated phthalocyanines containing nickel (NiTsPc) or copper (CuTsPc). The films were used as modified electrodes and displayed well-defined electroactivity, allowing their use as sensors for DA and AA.

## Experimental details

*O*-methoxyaniline (Aldrich) was distilled twice under a vacuum and stored in the dark at −10 °C. Hydrochloric acid (Vetec) and ammonium persulfate [$(NH)_4S_2O_8$, Vetec] were used as purchased. POMA in its emeraldine base form was chemically synthesized using the method described in [10]. The POMA powder was dissolved in dimethylacetamide (DMAc) under stirring for 12 h. The POMA/DMAc solution was filtered and slowly added to an HCl solution, pH 2.5, and then diluted to 2.0 g/l. The final pH was ca. 2.8. The procedures to obtain water-soluble POMA were adapted from those described in [7]. Poly(vinyl sulfonic acid; PVS), NiTsPc, and CuTsPc were purchased from Aldrich and used as received. The PVS and phthalocyanine anionic solutions were used at a concentration of 0.5 g/l and pH 2.5. All solutions were prepared with pure water from a Millipore system with a resistivity of 18.0 mΩcm.

POMA/NiTsPc and POMA/CuTsPc LbL films containing up to 20 bilayers were deposited onto hydrophilic glass, ITO-covered glass, and gold-covered glass substrates. The deposition of multilayers was carried out by immersing the substrates alternately into the polycationic (POMA) and anionic solutions for 5 min. After each deposition step, the films were rinsed in the washing solution (at pH 2.5) and dried with a $N_2$ flow. Film growth was monitored using UV-VIS absorption spectroscopy (Hitachi U-3000 spectrometer). Fourier transform infrared absorption spectroscopy (FTIR) analyses were carried out in films deposited onto Au substrates using a Nicolet 470 Nexus spectrometer, with the sample chamber purged with $N_2$ gas. The Raman scattering (Stokes) was obtained using the 514. 5-nm laser line with a Renishaw micro-Raman system In-Via, which is equipped with a Leica microscope (DMLM series) whose 50×-microscope objective lens was used to focus the laser beam onto a spot of ca. 1.0 $\mu m^2$.

Cyclic voltammograms were collected with LbL films deposited onto ITO using a potentiostat Autolab PGSTAT 30 Eco Chemie and a 10.0-ml, 3-electrode electrochemical cell. The reference electrode was an $Hg/HgCl/KCl_{(sat.)}$ (SCE); a 2.0-$cm^2$ platinum foil was used as auxiliary electrode, and the working electrode was the POMA/Phthalocyanine LbL film containing 3, 5, 10, 15, and 20 bilayers deposited onto ITO. The electrochemical response of POMA/NiTsPc films was studied as a function of the number of POMA/NiTsPc bilayers, pH of electrolytic solution, and scan rate. Detection of DA and AA was carried out in a HCl 0.1-M solution at concentrations varying from $1.41\times10^{-5}$ mol/l to $2.04\times10^{-4}$ mol/l at 50 mV/s. Cyclic voltammograms were also recorded in the presence of $6.7\times10^{-5}$ mol/l of DA and AA.

## Results and discussion

The UV-Vis spectra of POMA, CuTsPc, and NiTsPc aqueous solutions used for film fabrication are shown in Fig. 1. The POMA spectrum is characteristic of its doped state [11]; while for the CuTsPc solution, absorption bands at 610 and 690 nm were observed in the Q-band region assigned to dimeric and monomeric species, respectively [9, 12–14]. As the band at 610 nm was the most intense, one can infer that CuTsPc assumed preferentially the dimeric form in solution. A strong predominance of dimeric species was also observed in the NiTsPc solution, as revealed by the band at 624 nm, with only a small shoulder at ca. 660 nm indicative of monomeric species. Interestingly, when NiTsPc is assembled with POMA in the LbL films, adsorption of the monomeric species seems to be more effective. The latter is indicated in the absorption spectrum of the 20-bilayer POMA/NiTsPc film shown in the inset of Fig. 1, where there is preferential growth of the band at 675 nm, characteristic of the monomeric species. A similar effect was reported by Zucolotto et al. [9].

The sequential growth of the LbL films was monitored via UV-VIS absorption spectroscopy, and the results are shown in Fig. 2. An almost linear increase was observed for films containing PVS, CuTsPc, and NiTsPc as anionic species and POMA as cationic species after the absorption at 630 nm, which points to the same amount of material being adsorbed at each deposition step. As far as film fabrication is concerned, the use of POMA as the cationic polyelectrolyte is advantageous, resulting in a more effective adsorption in comparison with a conventional

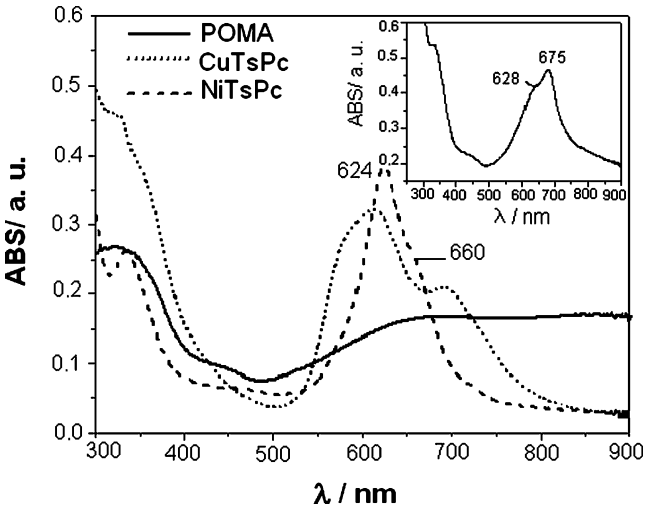


**Fig. 1** Electronic absorption of the aqueous solutions employed in film fabrication. Inset: electronic absorption of the 20-bilayer POMA/NiTsPc LbL film

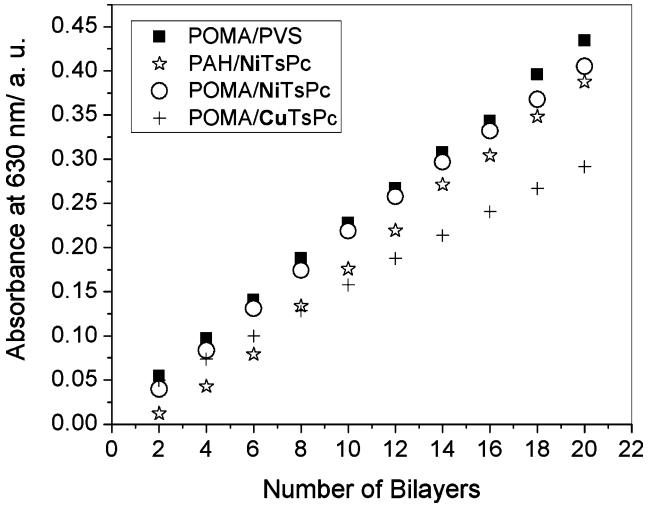


**Fig. 2** Increase of the absorbance at 630 nm as a function of the number of bilayers for the POMA-based and PAH/NiTsPc LbL films

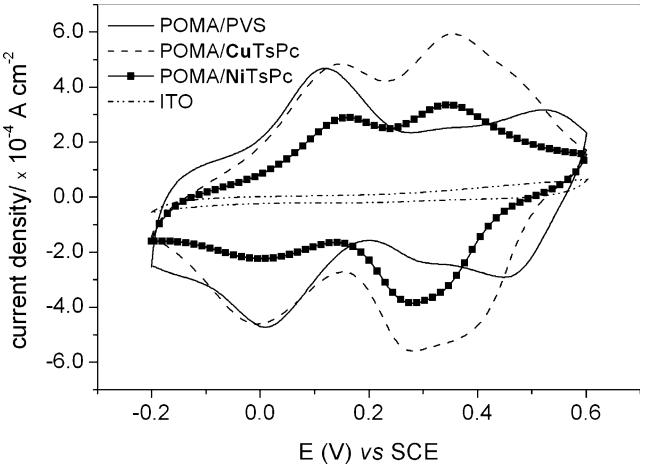


**Fig. 3** Cyclic voltammograms for a 50-bilayer LbL film from POMA/PVS, POMA/CuTsPc, and POMA/NiTsPc in a 0.1-M HCl solution at 50 mV $s^{-1}$

polyelectrolyte, namely, poly(allylamine hydrochloride; PAH), as indicated. Any explanation for the higher adsorption efficiency exhibited by the POMA-NiTsPc films is not straightforward. In this case, however, the methoxy groups from POMA may interact with adjacent layers of POMA via H-bonding (in addition to the electrostatic interactions that occur between POMA and NiTsPc), improving multilayer adsorption. The vibrational analysis through FTIR and Raman spectroscopies (not shown) for POMA and NiTsPc cast films and 20-bilayer POMA/NiTsPc LbL films point to differences not only in the relative intensities but also in the wave numbers. The latter suggests that the spectrum of the LbL film is not a simple superposition of the spectra from POMA and NiTsPc thus indicating chemical interaction between POMA and the phthalocyanine. The same applies to the LbL film made with POMA and CuTsPc.

The electrochemical properties of 50-bilayer POMA/PVS, POMA/CuTsPc, and POMA/NiTsPc LbL films are illustrated in the cyclic voltammograms of Fig. 3, obtained at 50 mV/s in HCl 0.1 M. For comparison, the voltammogram for a bare ITO electrode is also shown. The electrochemical response of the films containing phthalocyanine differed from that of a POMA/PVS film (used as reference). For the latter film, the redox pair at ca. +122 and +12 mV corresponds to the interconversion between the oxidation states leucoemeraldine (insulating, transparent yellow) and emeraldine (conducting, green) [7]. The bare ITO substrate has no electrochemical response in the potential range used here. Because of the well-known stability of NiTsPc LbL films [15, 16], this system was used in further experiments to investigate the influence of parameters such as the number of bilayers, pH of the electrolytic solution, and scan rate on the electrochemical properties. It is important to note that the POMA-TsPc films were stored at room temperature (24 °C) for several days or even weeks without loss of electroactivity.

Figure 4a shows cyclic voltammograms for POMA/NiTsPc LbL films with different thickness. The typical

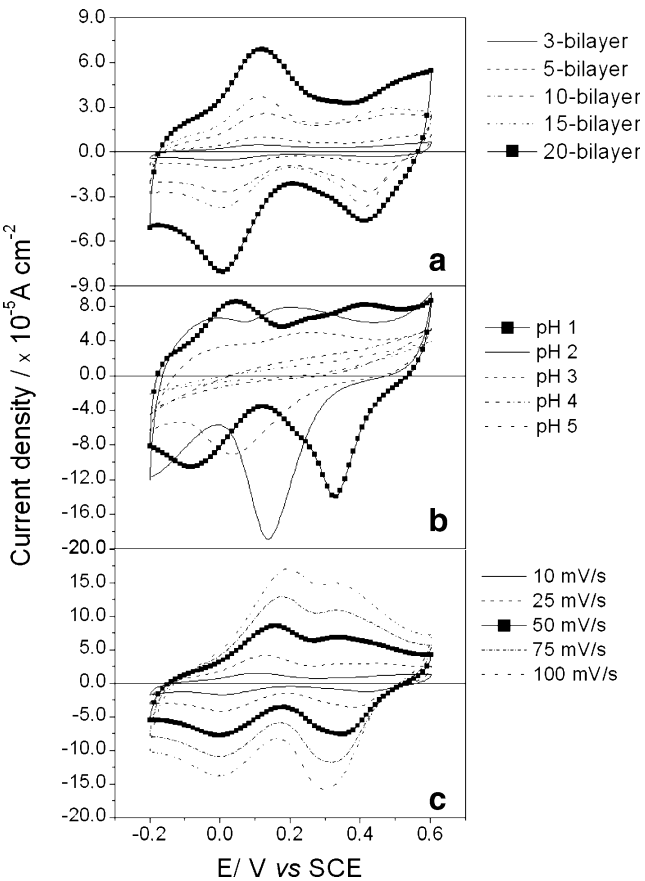


**Fig. 4** **a** Cyclic voltammograms for an LbL film from POMA-NiTsPc with various numbers of bilayers in a 0.1-M HCl solution at 50 mV $s^{-1}$. **b** Cyclic voltammograms for a 20-bilayer LbL film from POMA-NiTsPc at different pHs at 50 mV $s^{-1}$. **c** Cyclic voltammograms for a 20-bilayer LbL film from POMA-NiTsPc in a 0.1-M HCl solution and different scan rates

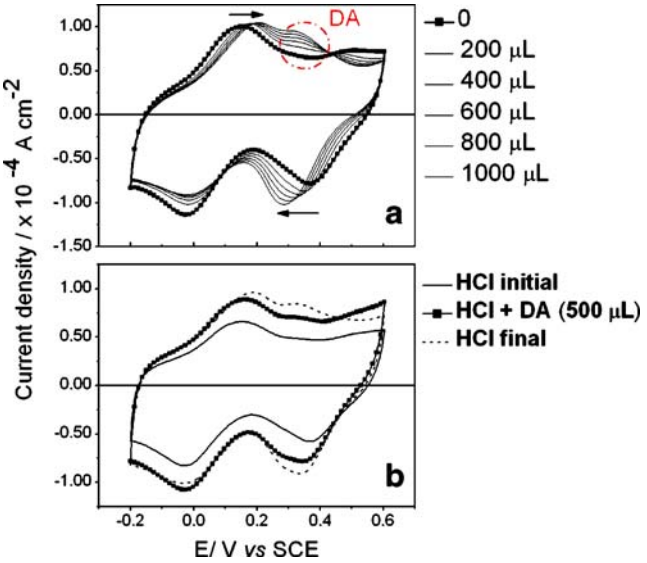


**Fig. 5** **a** Cyclic voltammograms for a 20-bilayer LbL film from POMA/NiTsPc in a 0.1-M HCl solution and POMA/NiTsPc in a 0.1-M HCl solution in the presence of DA at concentrations ranging from $2.77\times10^{-5}$ M to $1.76\times10^{-4}$ M (1,000 µl; from *bottom* to *top*). **b** Cyclic voltammograms for a 20-bilayer LbL film of POMA/NiTsPc in the absence and presence of $6.7\times10^{-5}$ M DA and again in HCl 0.1 M in the absence of DA. The changes in the electrode upon cycling with DA in the solution are not reversible. Scan rate, 50 mV/s

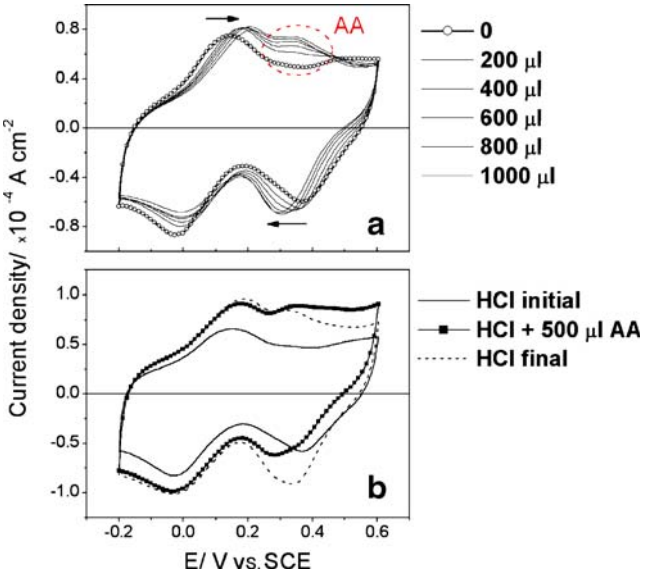


**Fig. 7** **a** Cyclic voltammograms for a 20-bilayer LbL film from POMA/NiTsPc in a 0.1-M HCl solution and POMA/NiTsPc in a 0.1-M HCl solution in the presence of AA at concentrations ranging from $2.77\times10^{-5}$ M to $1.76\times10^{-4}$ M (from *bottom* to *top*). **b** Cyclic voltammograms for a 20-bilayer LbL film of POMA/NiTsPc in the absence and presence $6.7\times10^{-5}$ M AA. Scan rate, 50 mV/s

POMA redox processes [17] can be visualized for a three-bilayer film, becoming more defined for thicker films. In none of the cases was the redox pair characteristic of film degradation noted, confirming the stability of POMA/NiTsPc LbL films. The pH of the electrolytic solution does affect the redox processes for POMA/NiTsPc, as shown in Fig. 4b. The cathodic peak shifts from −84 mV in pH 1 to +13 mV in pH 2, which is accompanied by a large increase in current. At pH 3 and above, the redox peaks were progressively poorly defined, and there was no electroactive response for the films at pH 4 or 5. Nevertheless, the electrochemical behavior

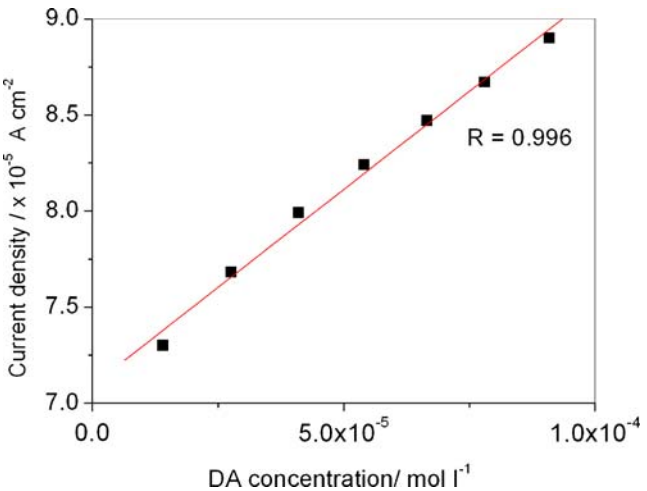


**Fig. 6** Peak current vs DA concentration for a 20-bilayer LbL film from POMA/NiTsPc in a 0.1-M HCl solution

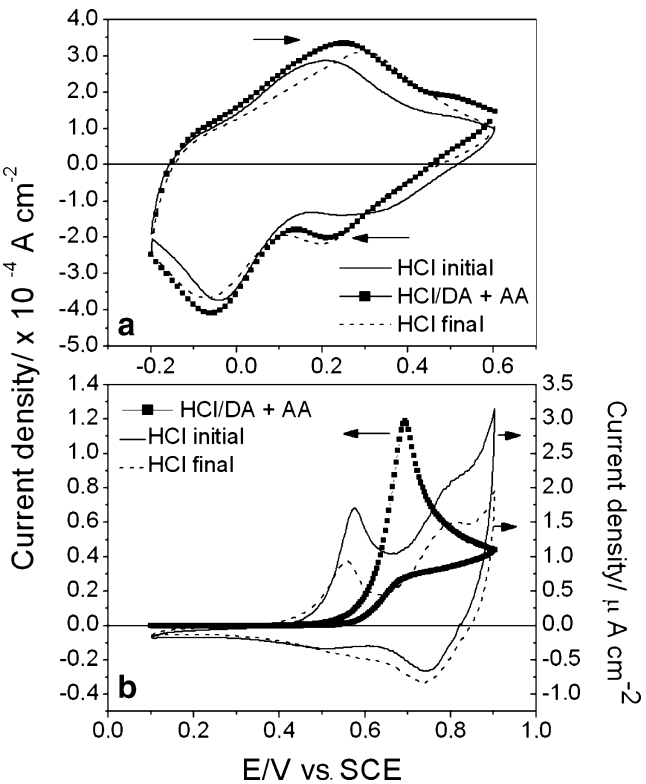


**Fig. 8** Cyclic voltammograms for 20-bilayer POMA/PVS (**a**) and PAH/NiTsPc (**b**) films in the absence and presence of $6.7\times10^{-5}$ M DA. The *dash-dot line* shows the electrochemical response of the film in HCl 0.1 M again after being scanned in the presence of DA. Scan rate, 50 mV $s^{-1}$

of the POMA/NiTsPc LbL films could be recovered by cycling the film at low pHs again.

The current density increased linearly with the scan rate in the range from 10 to 100 mV/s, as shown in Fig. 4c. In addition, the potentials at which the redox processes occur depend on the scan rate, especially for the first anodic process for the POMA/NiTsPc LbL film, shifting from +125 mV at 25 mV/s to +195 mV at 100 mV/s. This caused an overlap between the first and second anodic processes. We selected the rate of 50 mV/s for the remaining experiments because it led to a considerable current density and a good definition of the peaks. Therefore, for optimizing the parameters concerning the detection tests with DA and AA, we selected a 20-bilayer POMA/NiTsPc LbL film in HCl 0.1 M (pH 1) and a scan rate of 50 mV/s.

Figure 5a shows the cyclic voltammograms for a 20-bilayer LbL film from POMA/NiTsPc with various DA concentrations in the electrolyte solution. In addition to the typical POMA redox processes, an oxidation peak appeared at 340 mV, which is assigned to DA oxidation [18–21]. DA reduction was not observed, even at the highest concentrations used. Figure 6 shows the calibration curve for DA at the POMA/NiTsPc modified electrode where the current increases with DA concentration within the range from $1.41\times10^{-5}$ M to $1.0\times10^{-4}$ M. Saturation was observed for concentrations above $1.25\times10^{-4}$ M. The stability and reversibility of the modified electrodes were investigated, and the results are shown in Fig. 5b. The electrochemical response of the POMA/NiTsPc film changed irreversibly upon cycling in solutions containing DA. After employing the film in a DA-containing electrolytic solution, the oxidation peaked at 340 mV because DA oxidation still remained for a DA-free electrolytic solution. DA was trapped within the polymer matrix. It seems that the scan rate of 50 mV/s was sufficiently high for DA to enter the multilayers but not to leave them. The trapping of DA is also supported by the increase in current density for the POMA/NiTsPc LbL film after being cycled in a DA-containing HCl 0.1 M solution, which was maintained in the subsequent cycling with no DA in the solution.

Similarly to what was found for DA, the 20-bilayer POMA/NiTsPc LbL films were affected by the presence of AA in the 0.1 M HCl electrolytic solution (Fig. 7a), with an oxidation peak appearing at 340 mV because of AA oxidation. Again, no AA reduction was observed. The electrochemical response of the films was not reversible after cycling in an AA-containing solution, also pointing to trapping of AA in the POMA matrix (Fig. 7b).

To verify whether the trapping of DA or AA was due to POMA or NiTsPc, we performed subsidiary experiments with POMA/PVS and PAH/NiTsPc films, whose results are shown in Figs. 8a and b, respectively. After cycling in 0.1 M HCl containing $6.7\times10^{-5}$ M (500 μl) of DA or AA and then in solutions free of DA or AA, we noted that the response for POMA/PVS did not return to the original values. The latter may be an evidence that oxidized DA and AA species are somehow entrapped in the film matrix, for these species may interact via H-bonding with the $-OCH_3$ groups from POMA.

The shift in the oxidation peak for more positive potentials and the increased current—caused by cycling with DA or AA—were maintained when the measurements were taken again in 0.1-M HCl solutions with no DA or AA. In contrast, the response of the PAH/NiTsPc LbL films (Fig. 8b) was reversible. Upon cycling in HCl, these films displayed redox peaks typical of NiTsPc at 578 and 830 mV for oxidation and at 740 and 540 mV vs SCE for reduction. In the presence of DA or AA, these processes disappear, and an oxidation peak is seen at 693 mV, which is accompanied by a large increase in current. As the cycling was performed again in a 0.1-M HCl solution without DA or AA, the original electrochemical response was recovered. Furthermore, important to note is that the electrocatalytic effect towards DA oxidation was higher for POMA-NiTsPc electrodes (Fig. 5) in comparison to the PAH-NiTsPc modified electrodes.

## Conclusions

Nanostructured thin films containing Ni or Cu tetrasulfonated phthalocyanines were assembled in a multilayered fashion in conjunction with POMA. The films displayed a well-defined electroactivity, with redox pairs at 156 and 347 mV vs ESC characteristic of POMA. As expected, POMA/NiTsPc films presented a high electrochemical stability, which allowed their use as modified electrodes for detecting DA and AA at concentrations down to $10^{-5}$ M. Despite the high sensitivity exhibited by the POMA/NiTsPc system, the electrodes did not show reversibility because of absorption of DA or AA at the electrodes.

**Acknowledgements** This work was supported by FAPESP, FAPEPI, CNPq, CAPES and IMMP/MCT (Brazil).

## References

1. Oliveira ON Jr, He J-A, Zucolotto V, Balasubramanian S, Li L, Nalwa HS, Kumar J, Tripathy SK (2002) In: Kumar J, Nalwa HS (eds) Handbook of polyelectrolytes and their application. American Scientific, Los Angeles, pp 1
2. Huguenin F, Zucolotto V, Carvalho AJF, Gonzalez ER, Oliveira ON Jr (2005) Chem Mater 17:6739
3. Diab N, Oni J, Schulte A, Radtke I, Blöchl A, Schuhmann W (2003) Talanta 61:43
4. Parra V, Arrieta AA, Fernández-Escudero JA, García H, Apetrei C, Rodríguez-Méndez ML, De Saja JA (2006) Sens Actuators B 115:54

5. Coutanceau C, El Hourch A, Crouigneau P, Leger JM, Lamy C (1995) Electrochim Acta 40:2739
6. de la Fuente C, Acuña JA, Vázquez MD, Tascón ML, Gómez MI, Sánchez Batanero P (1997) Talanta 44:685
7. Cheung JH, Stockton WB, Rubner MF (1997) Macromolecules 30:2712
8. Decher G (1997) Science 277:1232
9. Zucolotto V, Ferreira M, Cordeiro MR, Constantino CJL, Moreira W, Oliveira ON Jr (2006) Sens Actuators B 113:809
10. Mattoso LHC, MacDiarmid AG, Epstein AJ (1994) Synth Met 68:1
11. Gonçalves D, Matvienko B, Bulhões LOS (1994) J Electroanal Chem (short communication)
12. Ferraldi G (1993) In: Leznoff CC, Lever ABP (ed) Phthalocyanines: propertiesandapplications,vol1.VCH,NewYork,pp291
13. Kobayashi N, Lever ABP (1987) J Am Chem Soc 109:7433
14. Zucolotto V, Ferreira M, Cordeiro MR, Constantino CJL, Balogh DT, Zanatta AR, Moreira WC, Oliveira ON Jr (2003) J Phys Chem B 107:3733
15. Siqueira JR Jr, Gasparotto LHS, Crespilho FN, Carvalho AJF, Zucolotto V and Oliveira ON Jr (2006) J Phys Chem B 110:22690
16. Crespilho FN, Zucolotto V, Siqueira Jr JR, Carvalho AJF, Nart FC, Oliveira ON Jr (2006) Int J Electrochem Sci 1:151
17. Gonçalves D, Mattoso LHC, Bulhões LOS (1994) Electrochim Acta 39:2271
18. Huang PF, Wang L, Bai JY, Wang HJ, Zhao YQ, Fan SD (2007) Microchim Acta 157:41
19. Wang Q, Jiang N, Li N (2001) Microchem J 68:77
20. Oni J, Nyokong T (2001) Anal Chim Acta 434:9–21
21. Ferreira M, Dinelli LR, Wohnrath K, Batista AAA, Oliveira ON Jr (2004) Thin Solid Films 446:301